UPTEC W05 015
Examensarbete 20 p
15 February 2005

# Advective Sediment Modelling with Lagrangian Trajectories in the Baltic Sea

Hanna Kling

## Abstract

**Advective Sediment Modelling with Lagrangian Trajectories in the Baltic Sea**
*Hanna Kling*

A model that calculates Langrangian water trajectories has been modified to handle sedimentation and resuspension and applied to the Baltic Sea. By adding a settling velocity and a mass to the water trajectories in the original model, they assume the properties of sediment particles. The particles are advected in the velocity field originating from a circulation model and follow the currents while they sink. The resuspension is induced by the orbital water velocity at the bottom due to surface waves. The particles keep moving until the water velocity is too low for resuspension to occur.

The new model shows good potential in calculating the final positions of light particles such as clay and fine silt. Animations of the travel routes indicate that the particles follow known circulation patterns in the Baltic. Larger particles, which are transported shorter distances in relation to the resolution of the model grid, are less suitable for modelling in this setting. Some of the approximations in the model are quite crude and to achieve a better description of the processes involved the next step will be to couple the model with a wave model.



Keywords: Lagrangian trajectories, sediment modelling, advective, Baltic sea, sedimentation, resuspension



## Referat

**Sedimentationsmodellering med advektiva vattentrajektorier**
*Hanna Kling*

En befintlig modell som beräknar Lagrange-trajektorier för vattenrörelser har modifierats till att kunna hantera sedimentation och resuspension, och har testats för Östersjön. Genom att ge vattentrajektorierna i ursprungsmodellen en massa och en sjunkhastighet antar de egenskaperna hos sedimentpartiklar. Dessa advekteras i hastighetsfältet från en cirkulationsmodell och följer vattenströmmarna medan de sjunker. Resuspensionen induceras av vattnets rörelser från ytvågor. Sedimentpartiklarna fortsätter att röra sig tills vattenhastigheten är för låg för att ge någon resuspension. Den nya modellen möjliggör storskalig sedimentmodellering och animering av transportvägar. Resultaten ser mycket lovande ut för små partiklar som lera och finsilt.



Nyckelord: Lagrange, trajektorier, sedimentationsmodellering, advektiva, Östersjön, sedimentation, resuspension

*Department of Eart Sciences*
ISSN 1401-5765

## Preface

The supervisors of this Master of Sience Thesis Work have been Kristofer Döös at the Department of Metheorology at Stockholm University and Andreas Gyllenhammar at the Department of Earth Sciences, Uppsala University. I want to thank Kristofer and Andreas, and also Peter Lundberg at MISU, for all their help and support, and all the people at MISU who has made these months a fun and rememberable time. Thank you to you all!!

Copyright © Hanna Kling and Department of Earth Sciences, Uppsala University.
UPTEC W05 015, ISSN 1401-5765
Printed at the Department of Eart Sciences, Geotryckeriet, Uppsala University, Uppsala, 2005.

# Contents

.

# 1 INTRODUCTION

Sedimentation modelling has become increasingly important as the pollution load entering the oceans with the riverine sediments has grown. Modelling sediment transport with advective trajectories is a new way of gaining knowledge in this field of study, and has the potential to become a versatile tool for sedimentation modelling.

## 1.1 TRAJECTORY MODELLING

A trajectory is the path of a point that moves in space. The term Lagrangian comes from the French mathematician Joseph-Louis Lagrange and refers to a way of describing the item studied and its surroundings. In a water transport setting the observer watches the world evolve around herself while she is traveling along with the fluid particle. The opposite perspective is the Eulerian view, where a fixed point in space is chosen and the evolution of time-dependent variables at this point is studied.

A trajectory can represent a particle of water or air, an object such as a hot air balloon (Draxler, 1996), a tracer molecule (Samson, 1980) or a hail stone (Heynsfield, 1983). By associating each trajectory with a fixed volume transport it is possible to calculate mass transport (Döös, 1995, Döös et al., 2004) and the trajectories can be used as a way of predicting the behavior and properties of masses of air and water. Formerly constructed by graphical means on maps, trajectories are nowadays usually computed numerically from gridded velocity fields obtained from Global Circulations Models (GCM). Trajectories in the atmosphere are based on the velocity of the winds, and trajectories in the ocean are based on the movement of the water masses.

Several methods for the construction of trajectories have been developed (Seibert, 1992). The use can be anything from predicting the future path of a violent storm or tornado (Wu and Wang, 2003) or mapping the circulation pattern of deep water in the oceans (Döös, 1995) to describing long-range transport of air pollutants in the atmosphere (Pack et al., 1978). Trajectory modelling has also proved to be a useful tool for establishing source-receptor relationships of air pollutants (Stohl 1996b).

## 1.2 SEDIMENTATION AND RESUSPENSION

Sedimentation and resuspension are controlling factors of the productivity in shallow-water ecosystems, through water enrichment by nutrients originating from the sediment. This input is related to desorption of nitrogen and phosphorus from resuspended particles and from mixing of pore-water nutrients into the water column (Simon, 1989). Resuspension might also be responsible for transport of sediment-bound nutrients from shallow to deeper waters in coastal areas (Håkanson and Floderius, 1989). A consequence of this relocation of nutrients can be enhanced phytoplankton growth during the summer season. In other regions the resuspension may lead to normal nutrient concentrations where the terrestrial supply of nutrients is cut short due to better waste water treatment.

Excess nutrients can be considered as pollutants, and together with heavy metals and other polluting substances a large fraction of them enter the sea by the river run-off. This riverine load of pollutants consists of pollution from different sources within the rivers catchment areas, such as industrial plants, municipal waste water treatment plants, farmland and managed forests, as well as natural background load. The polluting substances can be transported

long distances with the sediments, and thus knowledge of the sediment distribution in some ways represents knowledge of the distribution of the pollutants.

### 1.2.1 SEDIMENTATION MODELLING

Most sedimentation modelling undertaken today is small-scale and focused on detailed calculations of the governing physical processes. This may limit the range of the model to a smaller area, such as a small bay or a sound, since the spatial scale of the processes is very small and requires high resolution to model them properly. In return a very accurate description of the events can be obtained. The cost of making a model cover larger areas is cruder approximations, and thereby loss of detail.

The concept of modelling sedimentation with advective water trajectories is based on the idea that the sediment particles follow the water movement while they fall towards the bottom. If this water movement can be modelled properly, then the final positions of the sediment load should be close to reality as well. The water trajectory model used to calculate the water movements has proved to be useful in a number of applications, e.g. studies of the water mixing and overturning times in the Baltic Sea (Jönsson et al., 2004, Döös et al., 2004), see figure 1. The sedimentation model based on this trajectory model shows good potential of becoming a useful tool for large scale modelling.

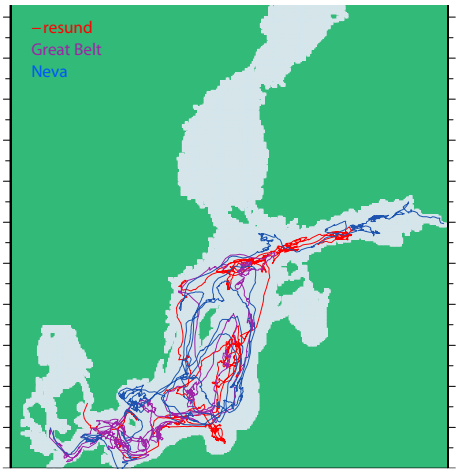


Figure 1: Water trajectories from Neva, Öresund and Great Belt in the Baltic Sea generated with the model made by Döös.

## 1.3 AIM OF THE DEGREE PROJECT

The aim of this project is to examine the possibility of large scale modelling of sediment transport with advective water trajectories. As a basis for the sediment model an existing trajectory model, assembled by Kristofer Döös at the Department of Meteorology at Stockholm University, is used. The sediment model is run with velocity field data from the Baltic Sea. The results are compared with sediment maps and the potential of the new model is evaluated.

# 2 BACKGROUND

The concept of this sedimentation model is to merge model data for the advective circulation patterns of water with sedimentation theory. To make the comprehension of the model easier a short theory background is presented, focused on the origin of velocity fields used and the basic concepts of sedimentation and resuspension.

## 2.1 OCEAN MODELLING

### 2.1.1 GLOBAL CIRCULATION MODELS

The ancestor of most numerical ocean models today is the Bryan-Cox-Semtner circulation model. The initial version was developed by Bryan (1969) at the University of Princeton in the 1960's. During the years that followed contributions to the model were made by Semtner (1974) and Cox (1984), and the model became widely accepted in the oceanographic community. A recent successor is the OCCAM model (Webb et al., 1998), developed at the Southampton Oceanography Centre. An offspring of the OCCAM model, particulary aimed at the Baltic Sea, is the Rossby Centre Ocean Model, to be described later.

### 2.1.2 GOVERNING EQUATIONS IN OCEAN MODELLING

The physical state of the ocean can in most cases be defined by the temperature, salinity and three components of velocity. In ocean models the potential temperature is generally used since this remains constant under adiabatic changes in the pressure. The salinity is a composite variable representing the combined effect of different dissolved salts in the ocean. With these variables, together with a continuity equation and boundary conditions, the evolution of the ocean can be specified using a momentum equation to give the change in velocity and an advection-diffusion equation for the changes of temperature and salinity (Webb, 1998).

The governing equations in the Bryan-Cox-Semtner model are the Navier–Stokes equations, subject to two simplifying approximations known as the Boussinesq and hydrostatic approximations (Pacanowski and Griffies, 2000). The Boussinesq approximation regards the ocean as incompressible, and replaces the density $\rho(x, y, z, t)$ with its average $\rho_0$, except in the gravitational force term. In the oceans the vertical density profile $\rho_0(z)$ usually does not vary more than 2 percent from its average value, and the assumption is thereby valid under most modelling conditions. The hydrostatic approximation implies that the vertical pressure gradient depends only on the density, i.e. $\partial p/\partial z = \rho(x, y, z, t)g$. The justification of this is based on scale considerations; the horizontal scale being much greater than the vertical. The resulting equations are called the 'primitive equations' (Bryan, 1969). The following formulation is taken from Webb et al. (1998). The horisontal momentum equation is

$$\partial \mathbf{u}/\partial t + (\mathbf{u} \bullet \bigtriangledown)\mathbf{u} + w\partial \mathbf{u}/\partial z + f \times \mathbf{u} = -(1/\rho_0)\bigtriangledown p + \mathbf{D}_u + \mathbf{F}_u. \quad (1)$$

Here $\mathbf{u}$ and $w$ are the horizontal and vertical velocity, $p$ is the pressure, $t$ the time and $f$ is the Coriolis parameter equal to $2\Omega \sin(\varphi)$, where $\Omega$ is the earth's rotation rate and $\varphi$ is the latitude. $\mathbf{D}$ represents the diffusion and $\mathbf{F}$ is a forcing term, here the shear stress of the wind on the sea surface.

The three dimensional advection/diffusion equations for the salinity $S$ and the potential temperature $T$ are

$$\partial S/\partial t + (\mathbf{u} \bullet \bigtriangledown)S + w\partial S/\partial z = \mathbf{D}_S + \mathbf{F}_S, \tag{2}$$

$$\partial T/\partial t + (\mathbf{u} \bullet \bigtriangledown)T + w\partial T/\partial z = \mathbf{D}_T + \mathbf{F}_T. \tag{3}$$

Here the forcing terms represent the precipitation and evaporation at the surface, $\mathbf{F}_S$, and the heat exchange at the surface, $\mathbf{F}_T$.
The pressure, incompressibility and density equations are

$$\rho g = -\partial p/\partial z, \tag{4}$$

$$\bigtriangledown \bullet \mathbf{u} + \partial w/\partial z = 0, \tag{5}$$

$$\rho = \rho(T, S, p). \tag{6}$$

The prognostic variables are the horisontal velocity, the potential temperature $T$ and the salinity $S$. From these the pressure, the vertical velocity and the density can be calculated.

### 2.1.3 THE BALTIC SEA AND THE RCO MODEL

The Baltic Sea is one of the worlds largest brackish water seas. It has an area of 377400 $km^2$, which corresponds to about 80% of the area of Sweden. The mean water depth is 56 metres and the maximum depth is 459 metres, at the Landsort Deep. The bottom topography is varied and divides the water masses into separate basins, the transport between them being limited by the high thresholds between. The narrow and shallow passages through the Great Belt and Öresund restrict the water exchange with the North Sea and thereby greatly influence the hydrography of the Baltic. Another pronounced feature is the seasonal sea-ice cover that modifies the air-sea exchange of momentum and heat during parts of the year (Meier and Faxén, 2001, Sjöberg, 1992).

The Baltic Sea drainage basin covers almost 750000 $km^2$ and comprises parts of 14 countries, see figure 2. Sweden, Finland, Poland and Russia represents the largest parts, close to 20 percent each. The drainage area is populated by 85 million people, even though less than one percent consists of urban areas. Almost 50 percent is forest land and more than 20 percent is arable land (Sweizer et al., 1996). Out of the riverine load of excess nutrients and heavy metals entering the Baltic sea the main share in both categories comes from the rivers Wisla, Oder and Nemunas (Helsinki Comission, 2004). Poland contributes with a big part of the total pollution load to the Baltic proper, but also has the largest population in the Baltic sea catchment area.

#### The RCO model

The Rossby Center Regional Ocean model (RCO) is a gridded 3D model that can handle the special features of the Baltic sea. It was developed at the Rossby Center, which is a part of the Swedish Meteorological and Hydrological Institute (SMHI), and is run at the Swedish National Supercomputer Centre in Linköping.

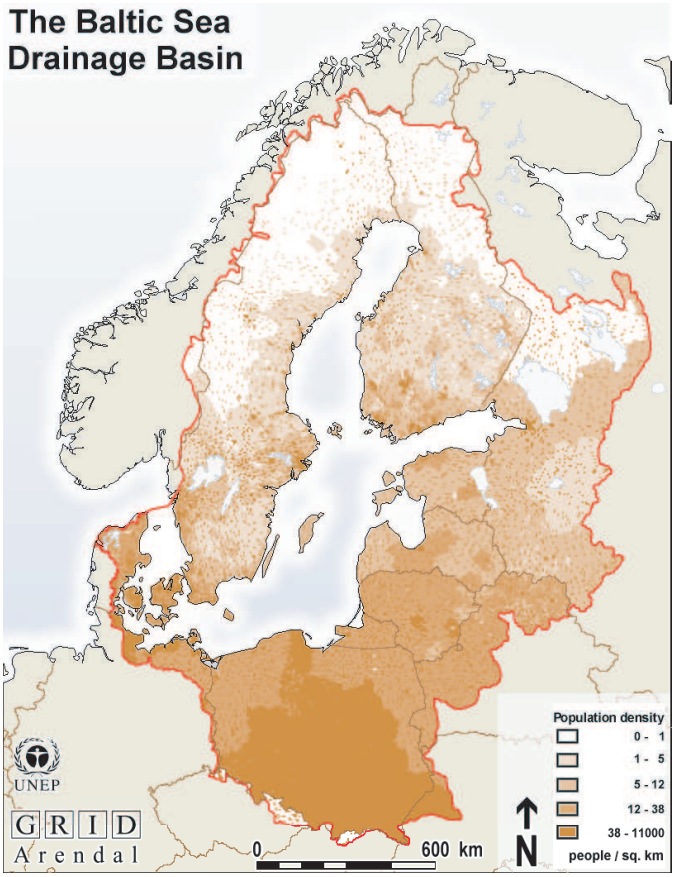


Figure 2: Population density in the Baltic drainage basin. Map from United Nations Environment Programme, www.grida.no/baltic/htmls/maps.htm

The domain of the RCO model is limited by an open boundary in the northern Kattegat. The velocity is zero on all solid boundaries, and the gradients of the potential temperature and salinity normal to the boundaries, including the bottom, are also zero (Webb et al., 1998). Surface boundary values of inflow, heat flux and wind speed are taken from observed climatological profiles and monthly river runoff data. The sea level elevation at the open boundary at Kattegat is prescribed from hourly tidal-gauge data (Meier and Faxén, 2001). The ocean model is coupled with a dynamic and thermodynamic sea ice model of the Hibler type (Hibler, 1979) that models ice thickness and air-sea heat flux characteristics by relating the strength of the ice interactions to the thickness and distribution of the ice.

**Model area and numerical implementation of the RCO model**

The model area ranges between 8 and 30 degrees longitude and 53 and 67 degrees latitude, which covers all of the Baltic Sea, figure 3. The spatial resolution of the grid used in this study are two nautical miles in the latitudinal y direction and four in the longitudinal x direction. One nautical mile is 1/60 of a degree, and one degree is defined as $2\pi R/360$. R is the earth radius, and the aproximate value for one degree is 111000 m. This gives

$\Delta y = (1/30) * 2\pi R/360 \approx 3667$ metres
$\Delta x = (1/15) * 2\pi R/360 * \cos(\varphi)$

where $\varphi$ is the latitude. The $\Delta x$ value varies since the distance between the meridians decreases northwards. The grid cells are almost quadratic since $\cos(60) = \frac{1}{2}$.

The model depths are based on realistic bottom topography data provided by the Baltic Sea Research Institute in Warnemünde, (Seifert et al., 2001). The domain is divided into 41 vertical levels with layer thicknesses varying from 3 metres at the surface to 12 metres at the deepest level. Within the upper 39 metres the layer thickness is constant. The maximum depth of the model is 250 metres (Meier and Faxén, 2001). The parts of the Baltic Sea with depths larger then 250 metres are few, small and have little impact on the flow, and are therefore excluded from the model.

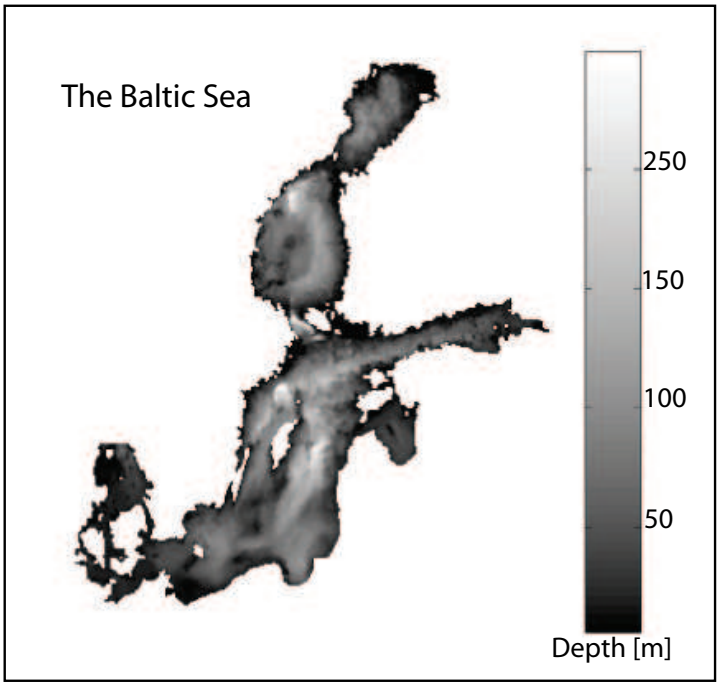


Figure 3: Bathymetry in the RCO model, from Seifert et al., 2001.

In the model area, conservation equations of momentum, mass, potential temperature and salinity are discretized horisontally on an Arakawa B-grid (Arakawa and Mesinger, 1976), figure 4, and calculated through finite differences. On a B-grid the cells overlap, and using a staggered grid is computationally efficient when centered difference equations are used.

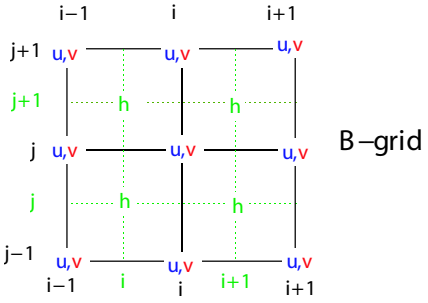


Figure 4: Arakawa B-gid

The zonal and meridional velocities $u$ and $v$ are calculated at the corners of the cells and the scalar quantities such as temperature, salinity and pressure at the center of each cell. The vertical velocity $w$ is not defined explicitly, but is calculated from $u$ and $v$ by conservation of cell volume.

## 2.2 SEDIMENTATION AND RESUSPENSION

### 2.2.1 SETTLING VELOCITY

Certain properties of the sediment load are fundamental for understanding the natural dynamics by which the sediment is transported and ultimately deposited. Density, size and the size distribution of the particles are controlling parameters affecting almost all physical properties of sedimentation and resuspension. The equations in this section can, if not otherwise stated, be found in Physics Handbook (Nordling and Österman, 1996), or similar. The theory presented here is the base for the approximations and estimations made in this study. Making the sedimentation model would have been an easy job if data on all the controlling parameters had been known. All theory here is not used directly in the model, but it may give perspective to the approximations later in this report.

**The drag force**

A particle falling in a fluid will accelerate under the force of gravity until it is balanced by the fluid drag and a vertical velocity $w_0$ is reached, which is constant relative to the surrounding water. The drag force $f_d$ is given by

$$f_d = \frac{1}{2} c_d a_2 D^2 \rho w_0^2, \tag{7}$$

where $c_d$ is the drag coefficient and $a_2 D^2$ is the projected area of the particle in the direction of the motion.

**The impelling force**

The gravitational force acting on the particle is counteracted by the buoyant force, given by Archimedes' principle. The difference between them is the impelling force

$$f_i = g(\rho_s - \rho) a_3 D^3, \tag{8}$$

where $(\rho_s - \rho)$ is the difference in density between the solid and the fluid, and $a_3 D^3$ is the volume of the particle.

**The settling velocity equations**

When the drag force (7) and the impelling force (8) balance, the settling velocity $w_0$ is found to be

$$w_0 = \sqrt{\frac{2a_3 D}{c_d a_2} \frac{\rho_s - \rho}{\rho} g}. \tag{9}$$

The settling velocity of particles has a basic relation to their size. Since it is not possible to account for all different shapes that particles can have, the "equivalent size" is used. That is the size of a quartz sphere having the same settling velocity as a less spherical natural grain, see figure 6 (Shepard, 1967). If the diameter of the equivalently sized sphere is denoted $d$,

then $a_2 D^2 = \pi d^2/4$ and $a_3 D^3 = \pi d^3/6$. This makes the fraction $a_3 D/a_2$ equal to $2d/3$ and equation (9) becomes

$$w_0 = \sqrt{\frac{4}{3c_d}\frac{\rho_s - \rho}{\rho} g d}\,. \tag{10}$$

**Reynolds number**

The drag coefficient, $c_d$, is a function of the Reynolds number and the particle shape. The Reynolds number is a dimensionless combination of variables that indicates the relative significance of the viscosity and inertia;

$$Re = \frac{\rho w d}{\mu}, \tag{11}$$

where $\mu$ is the dynamic viscosity of the fluid, figure 5.

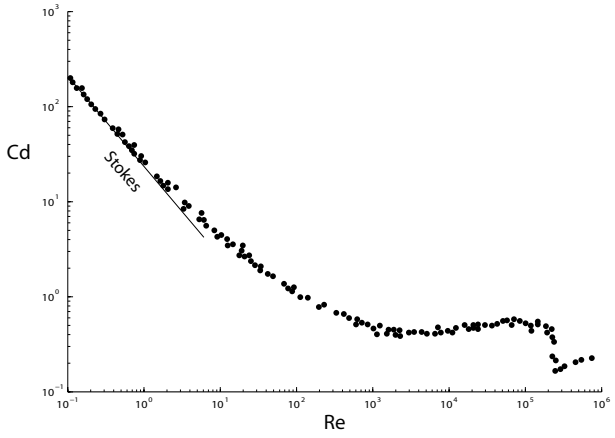


Figure 5: Relation between drag coefficients and Reynolds number for spherical particles, from Nielsen, 1992.

**Viscous settling**

There are two general modes of settling; viscous settling for particles smaller than about 0.2 mm and inertial settling for particles larger than about 2 mm. Between these sizes there is a transition zone. When $Re$ is very small the settling is said to be viscous since the viscous forces are much greater then the inertial forces. For viscous flow $c_d$ is equal to $24/Re$, and substituting this value into equation (10) yields the Stokes velocity

$$w_0 = \frac{\rho_s - \rho}{18\mu} g d^2\,. \tag{12}$$

This formula can be applied when $Re < 1$, which corresponds to an equivalent diameter of 0.2 mm and smaller. Since the viscosity $\mu$ is included in the equation, the viscous settling is temperature dependent (Shepard, 1967).

**Inertial settling**

If $10^3 < Re < 10^5$ the inertial force is the dominant. As can be seen in figure 5 $c_d$ is in this case approximately 0.5. This Reynolds number corresponds to particle diameters of 2 mm and bigger, (Shepard, 1967), and substituted into equation (10) the settling velocity becomes

$$w_0 \approx \sqrt{\frac{8}{3}\frac{\rho_s - \rho}{\rho} g d}. \tag{13}$$

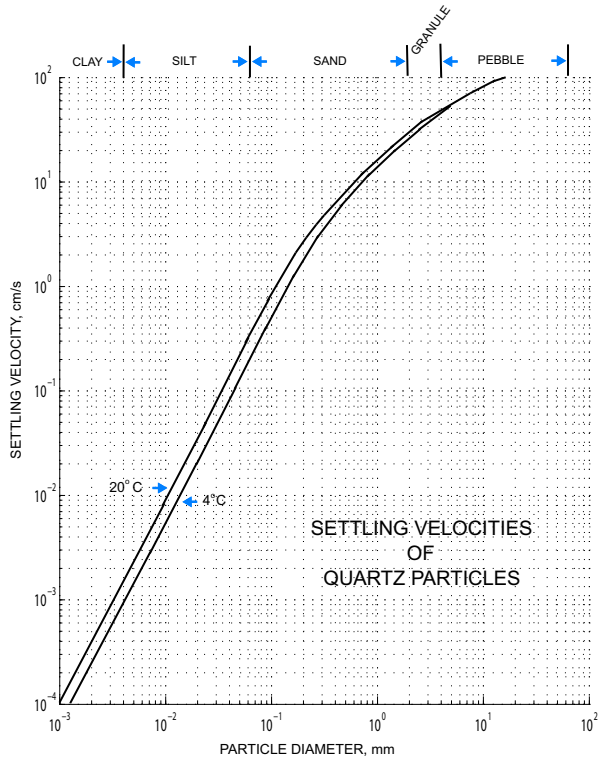


Figure 6: Settling velocity for quartz spheres, from Shepard, 1967.

**Empirical equations for settling velocity.**

There are several empirical formulae for the settling velocity. One applicable for spheres with diameters ranging from 0.063 mm to 10.0 mm was provided by Gibbs et al. (1971):

$$w_0 = \frac{-3\nu + \sqrt{9\nu^2 + gd^2(s-1)(0.003869 + 0.02480d)}}{0.011607 + 0.07440d}. \tag{14}$$

Here $\nu$ is the kinematic viscosity and $(s-1)$ is the difference in density between the particle and the fluid, normalized with respect to the fluid.

### 2.2.2 RESUSPENSION

Resuspension is the process whereby settled sediment material is brought back into the free water mass due to a shear stress on the bottom. Surface waves, storms and tidal currents are examples of phenomena that can cause bottom stress. Wave action is considered to be the most important factor in shallow water environments, such as coastal areas (Christiansen et al., 1997). As a result of the resuspension major areas of the central Baltic Sea with depths less than 70-80 metres are considered nondepositional over longer time scales, and it is estimated that more than 80% of the accumulated material in the deep basins originates from erosion of shallow water sediments (Jonsson et al., 1990). In the most shallow areas, where the depth is less than 3 metres, between 50% and 60% of the total sedimentation is resuspended material (Håkanson and Wallin, 1992).

**Entrainment of sediment**

The entrainment of a grain lying on the bottom occurs when the force exerted on the grain by the fluid exceeds the gravity force. The grain will then move by rolling, saltation, which is a form of jumping along the bottom, or by suspension, all depending on the flow velocity and the mass of the grain, figure 7.

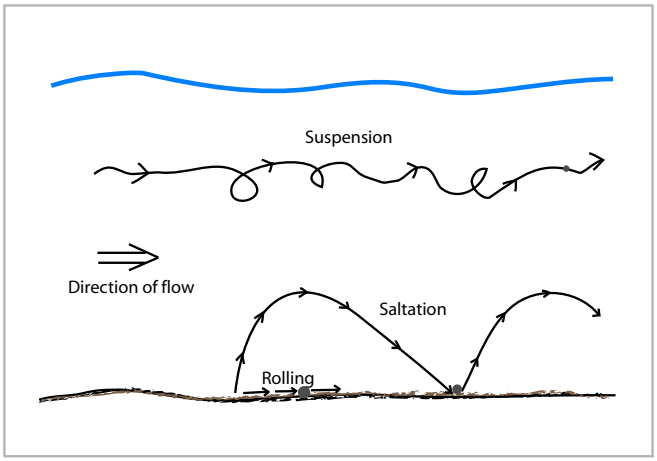


Figure 7: Different ways of travel for particles of different size.

When modelling resuspension one of two ways of describing the entrainment is generally used; bed shear stress or the near-bottom motion due to surface waves.

**The shear drag and the bed shear stress**

The threshold for entrainment is often expressed in terms of critical shear velocity or critical shear drag $u_{*cr}$. The shear drag is defined as

$$u_* = \sqrt{\frac{\tau_0}{\rho}}, \tag{15}$$

where $\tau_0$ is the bed shear stress. If $u_* \geq u_{*cr}$ entrainment will occur.

There are many ways, of various complexity, to describe the bed shear stress $\tau_0$. It arises from forces due to the water motion being slowed down by friction on the bottom. One basic way to describe it is by its relation to the flow velocity in the boundary layer;

$$\tau_0 = 0.5\rho_w f_w u^2. \tag{16}$$

The equation is known as the quadratic stress law, (Shepard, 1967). The frictional drag coefficient $f_w$ is of magnitude $10^{-3}$ and varies depending on the bottom type. The expression can also be stated in terms of e.g. particle diameter and spacing, vertical velocity profile or type of boundary layer. The relationships tend to be quite specific as to the conditions for their use.

**The near-bottom motion due to surface waves**

Another way of describing the threshold for entrainment is to relate it directly to the surface waves. The maximum horizontal orbital velocity associated with the oscillatory water motion created by the surface waves is

$$U_m = \frac{\pi a}{T \sinh(2\pi h/L)}, \tag{17}$$

where $a$ is the wave amplitude, $h$ the water depth, $L$ the wave length and $T$ the wave period. The velocity $U_m$ is then related to the equivalent diameter of the particles through an empirical relationship, and the flow velocity needed to entrain a particle can be found (Komar and Miller, 1973).

### 2.2.3 WAVES

Gravity waves are defined by the relationship between the wavelength $\lambda$ and the water depth $H$. If $\lambda \ll h$ the waves are independent of the depth and the water particles move in a circular orbits. The radii of the orbits decreases rapidly with depth. When $\lambda \gg h$ the waves are controlled by the depth and the water particles move in elliptic orbits. The longer the wave length the flatter the orbits becomes. When the wavelength is long compared to the depth the water motion is horizontal, figure 8.

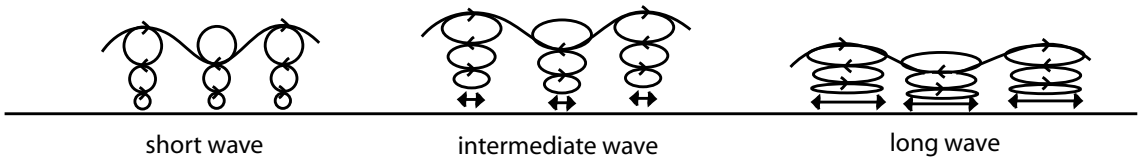


Figure 8: Water motion due to waves

Both short and long waves give rise to a shear stress when the movement is slowed down by the friction on the bottom in accordance with equation (15). However the shear stress due to the orbital motion of the short waves is greater than the one due to long waves.

**Waves in the RCO model**

The waves that give rise to water movements in the RCO model are mainly gravitational waves. The numerical size limit for these is a $\lambda$ equal to the length of two grid boxes, that is the smallest waves that are visible in the model. However these waves are very badly resolved, and in practice the smallest possible $\lambda$ is several grid box lengths. This means that only very long waves can be considered in the RCO model, and the short ones that are the origin of the orbital velocity at the bottom are absent.

# 3 METHOD

This section comprises descriptions of both a published model used to calculate water trajectories and a development of this model to deal with sedimentation and resuspension. To avoid confusion between them the existing model will be referred to as the water trajectory model and the new model as the sedimentation model.

## 3.1 THE WATER TRAJECTORY MODEL

The water trajectory model originates from Kristofer Döös at Department of Meteorology at the Stockholm University. It uses the velocity fields from the circulation models as input data, and calculates mass conservative trajectories. The model can follow a chosen water-mass both forwards and backwards in time from any section in the ocean (Döös et al., 2004). For the Baltic Sea it uses data from the RCO model (Meier and Faxén, 2001).

**Interpolation of the velocity field**

The horizontal velocities $u$ and $v$ at the corners of each grid box, and the vertical velocity $w$ at the top and bottom, are updated every second day from RCO-data, and the velocity field is interpolated linearly in time between these updates. The trajectories are then calculated analytically.

The velocity in each box is interpolated from the corners. The zonal velocity $u$ is found by averaging the meridional velocities $v$ and then interpolating zonally between the four corners of the box, viz.

$$u(x) = \frac{1}{2}(u_{i-1,j} + u_{i-1,j-1}) + \frac{x - x_{i-1}}{2\Delta x}(u_{i,j} + u_{i,j-1} - u_{i-1,j} - u_{i-1,j-1}). \tag{18}$$

Se figure 4 for i and j. By using $u(x) = \frac{dx}{dt}$ this expression can be written as the differential equation

$$\frac{dx}{dt} + \alpha x + \beta = 0, \tag{19}$$

where

$$\alpha = \frac{u_{i-1,j} + u_{i-1,j-1} - u_{i,j} - u_{i,j-1}}{2\Delta x},$$

$$\beta = \frac{x_{i-1}(u_{i,j} + u_{i,j-1} - u_{i-1,j} - u_{i-1,j-1})}{2\Delta x} - \frac{1}{2}(u_{i-1,j} + u_{i-1,j-1}).$$

The differential equation (19) for the zonal velocity, together with the boundary conditions $x(t_a) = x_a$ and $x(t_b) = x_b$, has the solutions

$$x_b = \left(x_a + \frac{\beta}{\alpha}\right) exp[-\alpha(t_b - t_a)] - \frac{\beta}{\alpha} \tag{20}$$

or

$$t_b = t_a - \frac{1}{\alpha} log \left[ \frac{x_b + \frac{\beta}{\alpha}}{x_a + \frac{\beta}{\alpha}} \right], \tag{21}$$

where $x_b$ is the zonal displacement and $t_b$ the associated time. The meridional and vertical trajectory displacements are calculated in the same manner and the times $t_b$ are compared (Döös, 1995). In other words: when a trajectory enters a grid box the time needed to reach a zonal, a meridional and a vertical wall of the box is calculated. Since the path is the same for all three calculations the shortest time $t_b$ tells where the trajectory will leave this particular box. This serves as the starting point for the next set of calculations, see figure 9. (In practice the equations are rewritten on a more complex dimensionless flow form to come to terms with the problem with non-square grid boxes due to changes in latitude. The interested reader is referred to Döös and De Vries, 2000.)

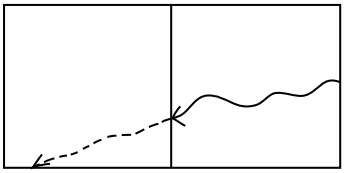

Figure 9: Trajectory path through a grid cell.

**Features of the water trajectories**

A water trajectory can only leave a grid box through the entry wall if the velocity field is updated while the trajectory is in the box. The trajectories will remain in the model domain until the simulation ends or they leave the Baltic through the Belts or Öresund. If a water trajectory reaches the top surface of the uppermost box, i.e. the sea surface, it will be reinserted in the box; it can not evaporate. Furthermore it can not reach the solid boundaries of the model domain due to the water mass conservation, i.e. there is no flux through the sea bottom.

The trajectories can be created all at once, or released over a longer period of time. The number of trajectories generated can be related to the volume of the flow or to the velocity of the flow. They can also be set to a fixed number.

The study of trajectories is of a statistical nature. The path of a single particle may seem haphazard and chaotic, and two particles that enter a simulation area next to each other will eventually diverge, no matter how close they are initially. It is not until a large number of trajectories has been studied that valid information can be extracted.

## 3.2 MODELLING SEDIMENTATION

A settling velocity $-w_{sed}$ is calculated and added to the vertical velocity $w$ in every grid box a sediment particle passes through. The velocity is dependent of the particle size according to equation (12) in section (2.2.1) for particle diametres up to 0.2 mm and the empirical equation (14) for larger particles.

The particles are considered to be spherical quartz grains. The diameter and density of the particle and the dynamic viscosity of the water needs to be specified at simulation startup.

The trajectories are programmed to leave the circulation, i.e. the calculation loop, and save their positions if they reach the floor of a bottom box.

## 3.3 MODELLING RESUSPENSION

The basic concept of the resuspension modelling is that a sedimented particle trajectory remains out of circulation until the horizontal velocity in the grid box where it hit the bottom reaches a critical value. Every time the program loops over the trajectories each trajectory either continues its course or, if it is out of the calculation loop, checks if the reentry conditions are fulfilled.

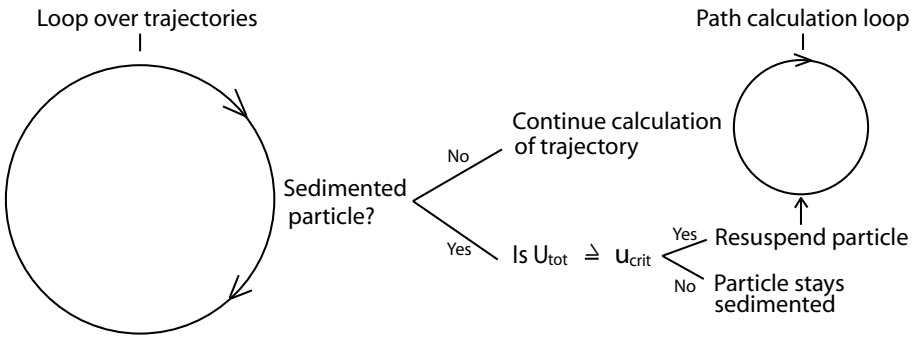


Figure 10: Illustration of the program process. The parameters $U_{tot}$ and $u_{crit}$ are defined in section 3.3.2

### 3.3.1 APPROXIMATION OF THE ORBITAL VELOCITY

The dominant force acting on a sedimented grain in a shallow water environment originates from the orbital velocity induced by short gravity surface waves. The waves give rise to a short-range back and forth movement in the bottom layer but does not lead to a net transport. This motion is not visible with the spatial resolution of the water trajectory model, and since it plays no part in the advection of the trajectories it is absent in the model. But when it comes to particle entrainment the motion is not negligible since this additional momentary velocity results in a proportionally larger shear stress than the velocity caused by longer waves. Hence most resuspension modelling is based on data of the surface wave field to make calculations of this shear stress possible. Since this information is not included in the water circulation model (RCO) an alternative way of representing the forces was needed. Any resuspension due to tides is neglected in this model since the tidal influence in the Baltic Sea is very small.

The velocity $u(x, z, t)$ of a surface gravity wave can, according to Mysak and LeBlond (1978), be described as

$$u(x, z, t) = \frac{agk}{\omega \cosh(kH)} \cosh[k(z + H)] \cos(kx - \omega t). \tag{22}$$

Here $a$ is the wave amplitude, $k$ the wave number, $\omega$ the angular frequency, $t$ the time and $H$ the water depth. At the bottom $z$ is $-H$ and $\cosh([k(z + H)])$ will be equal to one. The last factor of the equation, $\cos(kx - \omega t)$, varies between -1 and 1. Approximating the term with the value 1 will give a $u(x, z, t)$ that sometimes is too big, and the particles may remain

sedimented a shorter time than they otherwise would have been, but the final positions of the trajectories will be almost the same. The simplified equation will be

$$u(x,z,t) = \frac{agk}{\omega \cosh(kH)}. \tag{23}$$

In this equation the only parameters available from the model are $g$ and $H$. The angular frequency $\omega$ can be written as

$$\omega^2 = gk \tanh(kH) \tag{24}$$

Substituting $\omega$ with $2\pi/T$ and moving $g \tanh(kH)$ to the left hand side in this equation makes it possible to iteratively find a value of k, given a suitable $T$. Using these values for $k$ and $\omega$ in equation (23), and leaving the amplitude $a$ out, a value for a meta-parameter $u_{-a}$ can be calculated for each model depth $H$, see figure 11. The $u_{-a}$ parameter can then separately be scaled by an approximation of $a$. Separating $a$ and $u_a$ minimizes the calculations of the orbital velocity made in the main program since $u_a$ can be calculated at program startup.

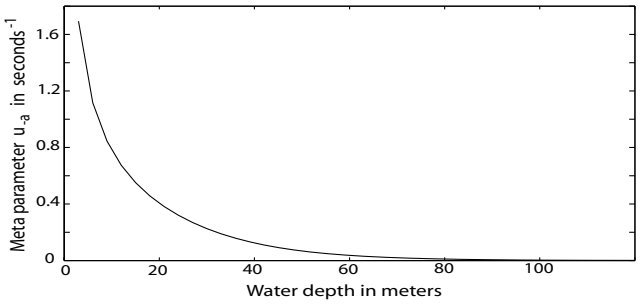


Figure 11: The meta parameter $u_{-a}$.

To approximate the wave amplitude, without any knowledge of the wave field, the water velocity was used. The velocities in the water trajectory model originates from RCO data. The RCO does not include a wave model, but is forced by wind data at the surface. Since short surface waves generally are wind-induced an approximation of the amplitude can be that it is proportional to the water velocity at the surface, $a = \alpha U(surface)$, where $\alpha$ is a real constant and $U = \sqrt{u^2 + v^2}$. Using a proper wave model would make these crude approximations unnecessary, but coupling the water trajectory model and a wave model was beyond the scope of this project.

### 3.3.2 IMPLEMENTATION

With a period $T$ specified at the start of the simulation a vector with the values of the meta-parameter $u_{-a}$ at the depth of the lower boundary of each of the 41 grid boxes is calculated and stored. A critical value $u_{crit}$ for the total horizontal velocity needed for particle entrainment and an $\alpha$ associated with the wave-amplitude approximation are also specified at startup. All input parameters can be seen in figure 12. Each time the program loops over the trajectories a trajectory can either be in circulation or be sedimented and thereby out of circulation. If the trajectory is sedimented an approximative total horizontal bottom velocity $U_{tot}$, from long waves and orbital movements from the short surface waves, is calculated:

$$U_{tot} = u_{-a}(bz)a + U(bz) = u_{-a}(bz)\alpha U(s) + U(bz). \tag{25}$$

Here $bz$ is the vertical grid box level at the bottom and $s$ is the surface grid box. The model distinguishes between the particle coordinates and the coordinates of the grid box it is in. If $U_{tot} \geq u_{crit}$ then the particle will be resuspended and put back into circulation. This is done by changing the vertical coordinate $z$ of the particle to be at the middle of the bottom box instead of on the lower boundary. The $x$ and $y$ coordinates are not changed and the particle is still in the same grid box. From the new position the particle trajectory will continue in accordance with the current velocity field.

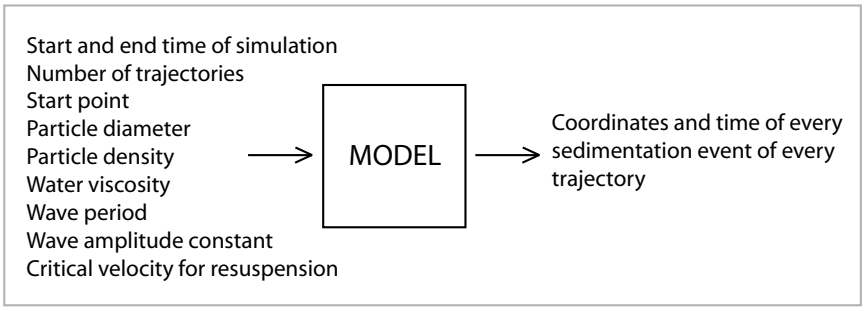


Figure 12: In and output of the sedimentation model.

### 3.3.3 APPROXIMATIONS OF PARAMETERS

**Wave period**

It has been shown by Jönsson (2001) that an average peak period is about 4 seconds in the Baltic proper. The peak period is $T_p = f_p^{-1}$ where $f_p$ is the frequency at the peak of the wave spectrum. A report from SMHI (Svensson and Wickström, 1986), with wave statistics from the the south cape of Öland in the central Baltic, indicates that a period of 8 seconds corresponds to waves near the upper end of the scale. This value of $T$ was chosen for estimating the wave number $k$ since it represents large "average" waves that are not storm waves.

**Wave amplitude**

Water velocities at the surface grid boxes were monitored during one-year simulations, starting at Wisla and Oder, to get a value of the surface velocity in the Baltic proper. The mean velocity, $\overline{\sqrt{u^2+v^2}}$ turned out to be between 4 and 5 cm/s. The velocities ranged between 0.5 cm/s and 12 cm/s. If a large wave, about 4 metres from crest to trough, corresponds to a surface velocity of 10 cm/s, then $\alpha \approx 20$, i.e. the amplitude $a$ is proportional to $20U$. According to FRP (1978) a typical value for the velocity of currents outside the coastal area is 10 cm/s to 20 cm/s.

**Critical velocity for entrainment**

The critical velocity $u_{crit}$ was taken from two sources. For frictional material, that is material without cohesive forces between the particles, the Hjulström curve (Hjulström, 1935) was used. Material the size of coarse silt and larger, $d \geq 0.02$ mm, was regarded as frictional, and the corresponding critical velocities are approximately 11 - 12 cm/s. For the cohesive material, a relationship due to Postma (1967) was used. The water content was considered to be 100 %, and the value for $u_{crit}$ is then 10 cm/s for the whole fraction.

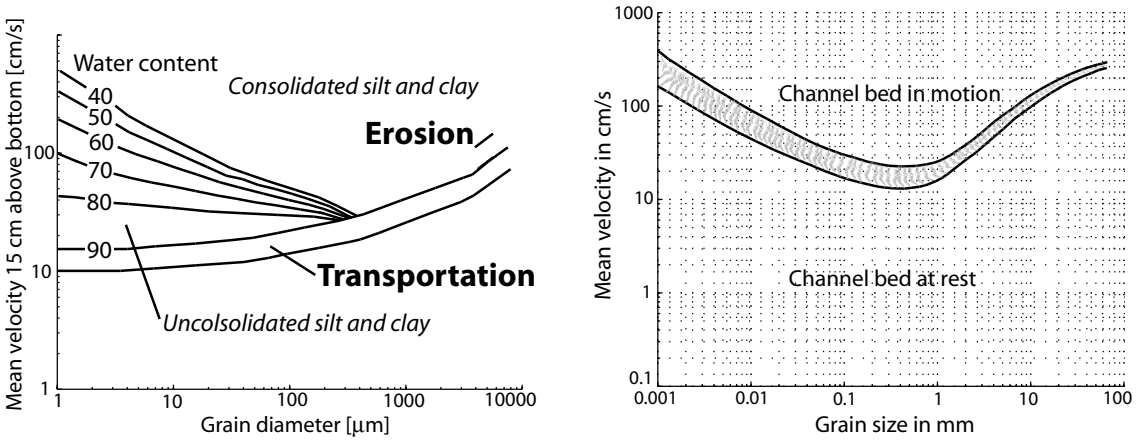


Figure 13: Critical velocity for entrainment. Figures from Postma, (1967) and Hjulström, (1935).

### 3.3.4 EXPERIMENTS

The Polish river Wisla in the Gdansk bay was chosen as model river. It is one of the largest of the rivers in the Baltic Sea drainage basin, and it contributes with a proportionally large share of the polluting substances entering the sea.
All simulations were made with Wisla as starting point.

**Sensitivity analysis**

To examine the model sensitivity to changes in the parameters a series of tests were performed. Two standard runs were used as comparison, only differing as to the particle diameter, see table 1. The diameters chosen were 0.006 mm, the smallest size of medium silt, and 0.003 mm, fine silt. The particle density was chosen to 2620 $kg/m^3$, the average density of pure quartz. The parameters that control the approximation of the orbital velocity in the bottom box, i.e. the period time T and the amplitude constant $\alpha$, were chosen to maximize $u_a(bz)a$ and thereby $U_{tot}$, see equation (25).

All runs were made with 500 trajectories released periodically during a year from Wisla, and the simulation was for a total of six years. It should be noted that the number of trajectories may be insufficient from a statistical perspective, but since each of the runs were made using exactly the same data every time they can still give a hint of the effects of changes in the parameters.

| | Standard | Standard 2 |
|---|---|---|
| diameter | 0.006 mm | 0.003 mm |
| particle density | 2620 $kg/m^3$ | 2620 $kg/m^3$ |
| $u_{crit}$ | 0.10 m/s | 0.10 m/s |
| period time T | 8 s | 8 s |
| $\alpha$ constant | 20 s | 20 s |
| water viscosity | $1040{*}10^{-6} Ns/m^2$ | $1040{*}10^{-6} Ns/m^2$ |

Table 1: Table of parameters for standard runs.

Tests were made with all parameters in the table except the diameters. For the period time T, the lower value mentioned in (3.3.3), T = 4 s, was tested. For $\alpha$ a lower value, $\alpha = 5$, was tested. This corresponds to a higher water velocity if the height of the waves are kept the same. Two lower values for particle density was tested, 1900 $kg/m^3$ and 1700 $kg/m^3$. These values are commonly used in practical studies when a mixture of fine sediments and water are considered, see for example Christiansen et al. (1997). There was also a test where the resuspension height, i.e. the distance from the bottom, was decreased. The standard case was 0.5 times the height of the bottom box, which generally implies that the particle is swept along with the currents 1.5 meters above the bottom. The test was for 0.1 times the height of the box. All these test were compared to the medium silt in the standard run. Different values for $u_{crit}$ were tested comparing to the fine silt in standard 2. Since the fine silt is a lighter particle than the medium silt any effects would be more visible. The values 0.08 m/s, 0.15 m/s and 0.20 m/s were tested.

The dynamic viscosity of the water was set to $1040 * 10^{-6} Ns/m^2$ which is the value for pure water at 291 K according to Physics Handbook (Nordling and Österman, 1996). When testing the influence of the water viscosity a simple stepwise change of the viscosity between tabular values was used. For example, all water temperatures below 2.5° C gave the same viscosity as 0° C, temperatures between 2.5 and 7.5° C were given the value for 5°C, and so forth. The salinity was ignored in this approximation. The varying viscosity was tested for both medium and fine silt.

**Runs with long time span**

30 years simulations with a vast number of trajectories were made. The particle sizes tested were clay with a diameter of 0.001 mm, and the fine silt used in Standard 2. The particles were released continuously during the first two or four years. Since the data set only comprises data for 12 years (starting 1980-05-28), the set was looped. To examine the impact of viscosity runs with and without varying viscosity were made.

A 20 year simulation with only 500 trajectories, all released during the first year, was also made to study the paths of the individual particles through the Baltic. This data was then used to make animations and snapshots in time.

**Reference material**

The sediment maps used for comparison are made by the Swedish Geological Survey, SGU, and the Lithuanian Geological Survey, LTG. The maps will be referenced as SGU/LTG in the figures.

# 4 RESULTS

## 4.1 LONG SIMULATIONS

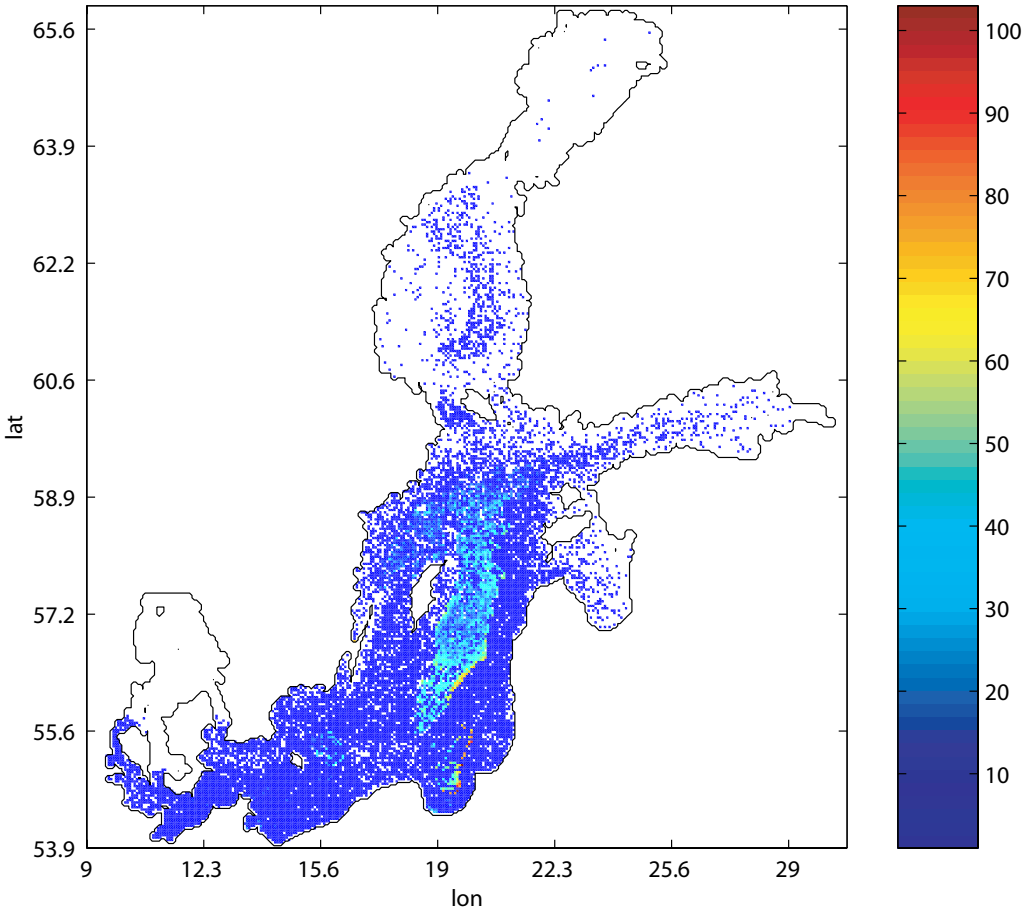


Figure 14: 85000 clay particles from Wisla after 30 years. The scale shows number of particles sedimented per grid cell.

**30-years simulations with clay**

The 30 years simulation from Wisla makes the particles spread out all across the Baltic. Since the changes in the velocity field make the trajectories behave chaotic this is an expected result; if there are enough particles they will end up everywhere. The grid cells with only a few particles in them can be considered as "noise" and if they are excluded the areas with numerous particles can be seen more clearly. In figure 15 all grid cells with 15 particles or less are emptied. The figure includes a map for comparison. The green area on the map is peltic mud and aleurit peltic mud, in which more than 70% of the particles and 50-70% of the particles respectively have a diameter less than 0.01 mm. The blue area is peltic mud with organic content. According to any particle size scale mud have a particle diameter of 0.002 mm or less, not 0.01, but this is the finest fraction shown on the map. Note that the pattern on the map is the result of sedimentation from many rivers around the Baltic, and not just Wisla.

The areas with clay in the simulation figure shows good resemblance to the map, and also to a figure of the bottom topography where only the areas with depths greater than 90 metres are shown, figure 16.

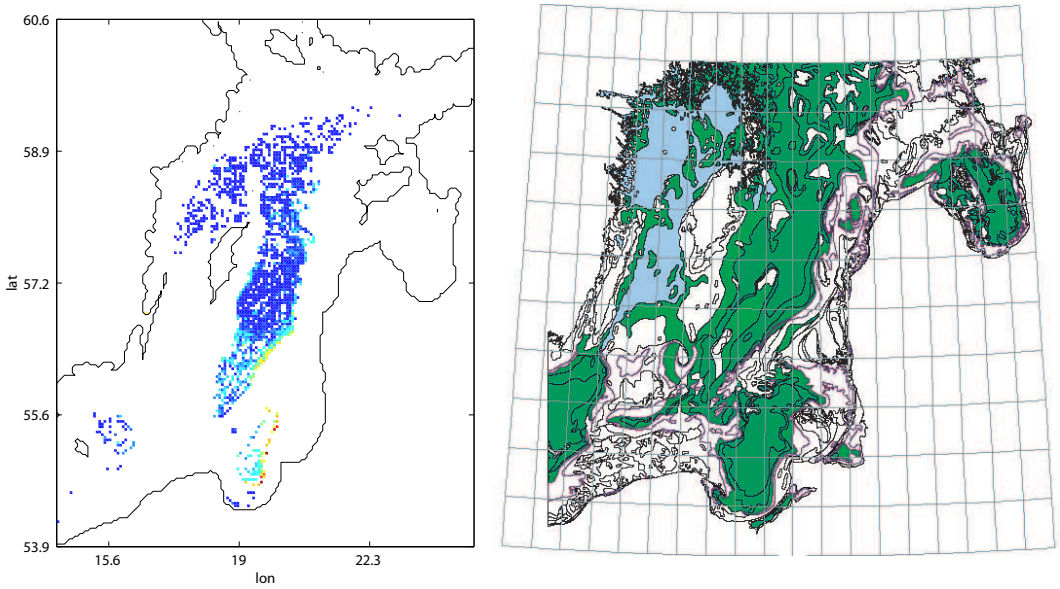


Figure 15: Grid cells with number of particles $\geq$ 16 compared to sediment map from SGU/LTG showing areas with particle sizes less than 0.01 mm.

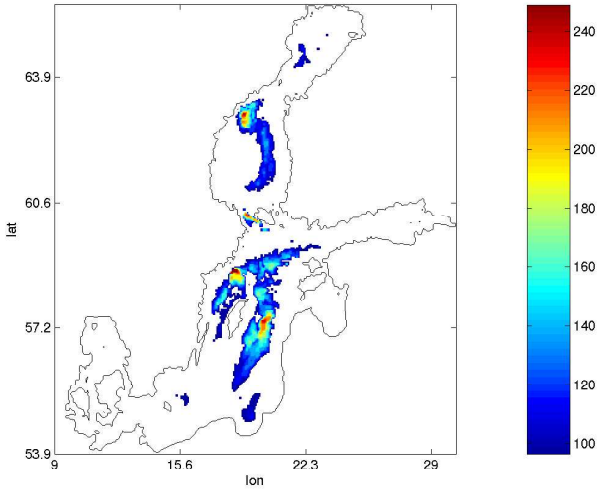


Figure 16: Bottom topography for areas with depths greater then 90 metres. The scale shows depth in meters

The large 30 year simulation with clay, seen in figures 14 and 15, was made without varying viscosity. To examine the effect of the viscosity on long simulations two runs were made with 47500 particles, with and without varying viscosity. The final results were almost identical.

**Snapshots in time**

The behavior of the particles was examined through animations of the positions during 20 years. Snapshots from the animations can be seen below. During the first two years the particles travel close together along the western shore of the Baltic Proper, spread out in the area north of Gotland and then continues south down the eastern shore of Sweden. After about three years the particles are spread evenly through out the Baltic and then slowly start to gather again in the areas where they are to be found after a long time has passed.

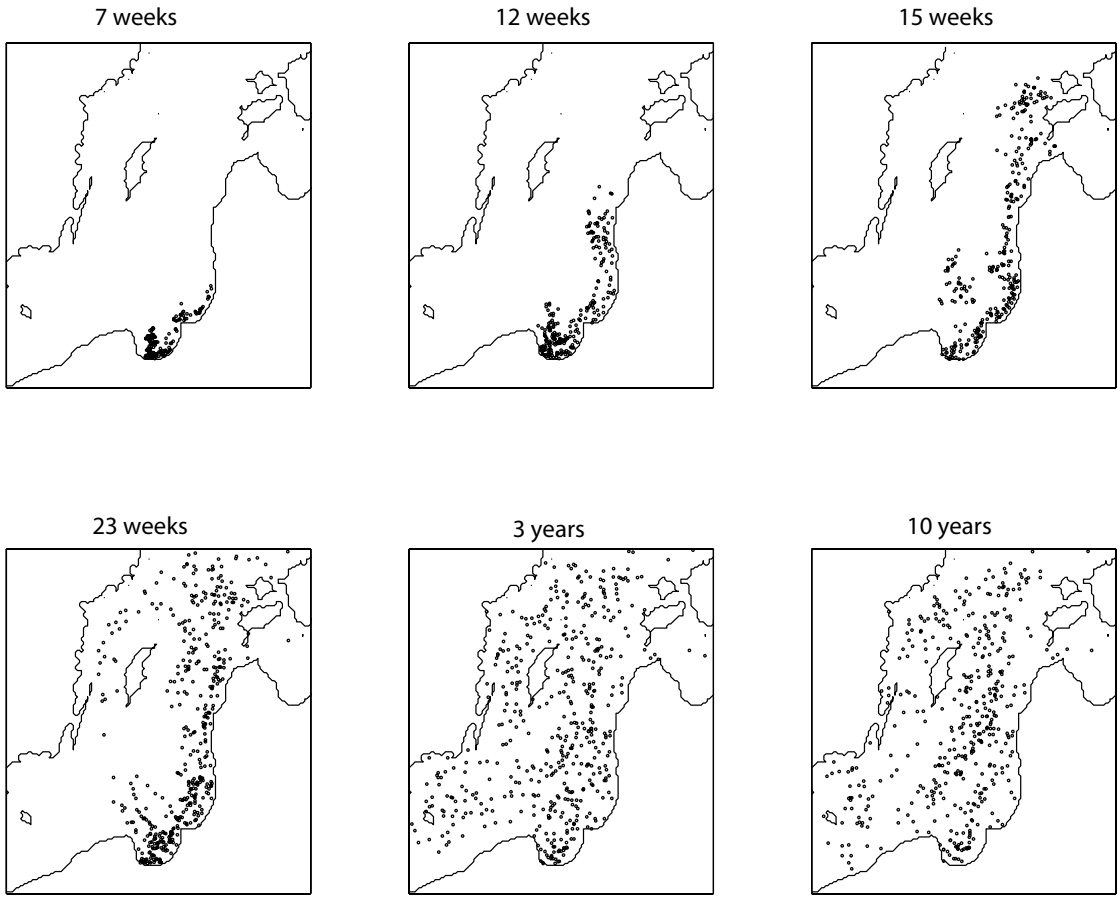


Figure 17: Positions of 500 clay particles at different times during a 20 year simulation.

**30-years simulations with fine silt.**

The simulation with fine silt was made with 47500 particles and varying viscosity. Figure 18 shows the outcome with and without exclusion of grid cells with less than 6 particles. The result was compared with a run without varying viscosity and there was no visible difference between the two. A map from SGS/LGS in figure 19 shows the actual sediment distribution in the area.

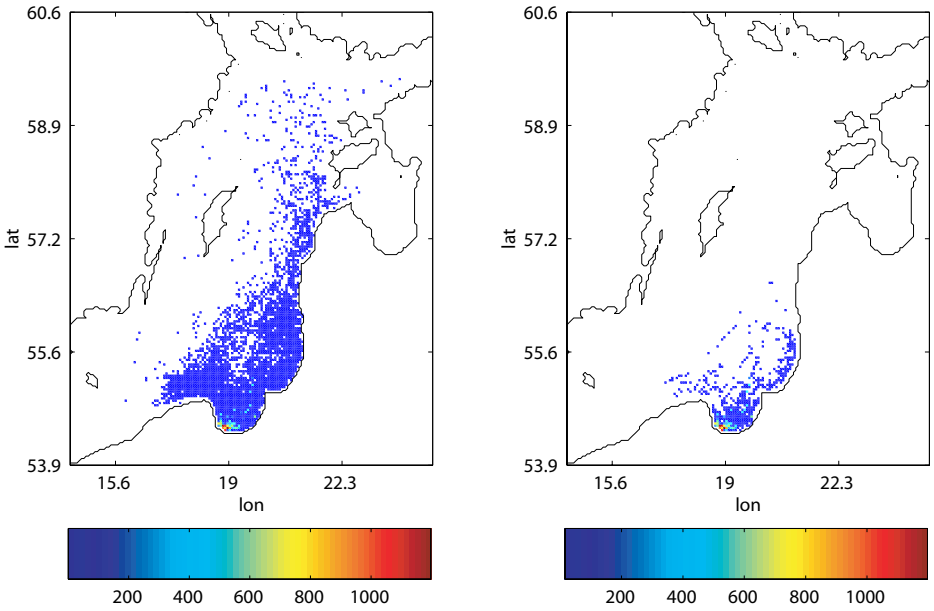


Figure 18: 47500 particles of fine silt after 30 years. The scale shows number of particles sedimented per grid cell. The right figure shows grid cells with number of particles $\geq 7$.

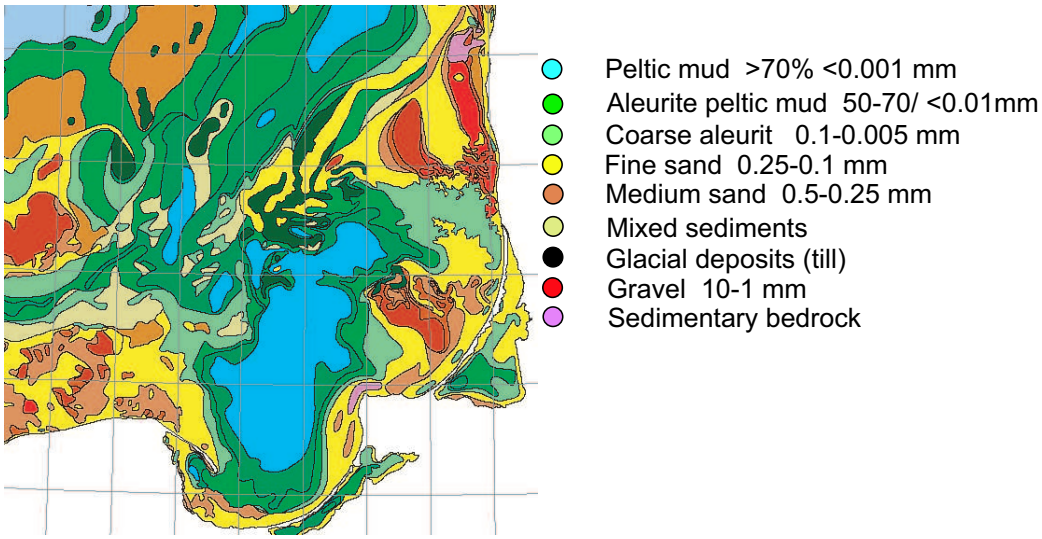


Figure 19: Sediment map over the south east corner of the Baltic proper, from SGU/LTG.

A comparison between the modelled result and the map shows that the silt particles did not deposit in the areas mapped as peltic and aleurit peltic mud to the same extent as the clay did.

## 4.2 SENSITIVITY ANALYSIS

**Experiments with medium silt**

Changing the parameters controling the approximation of the orbital velocity in the bottom box, i.e. the period time T and the amplitude constant $\alpha$, did not exert much influence on the final result. The particles traveled a somewhat shorter distance, but the results of the three tests, with T = 4, $\alpha = 5$ and T = 4 & $\alpha = 5$ respectively, did not differ much.

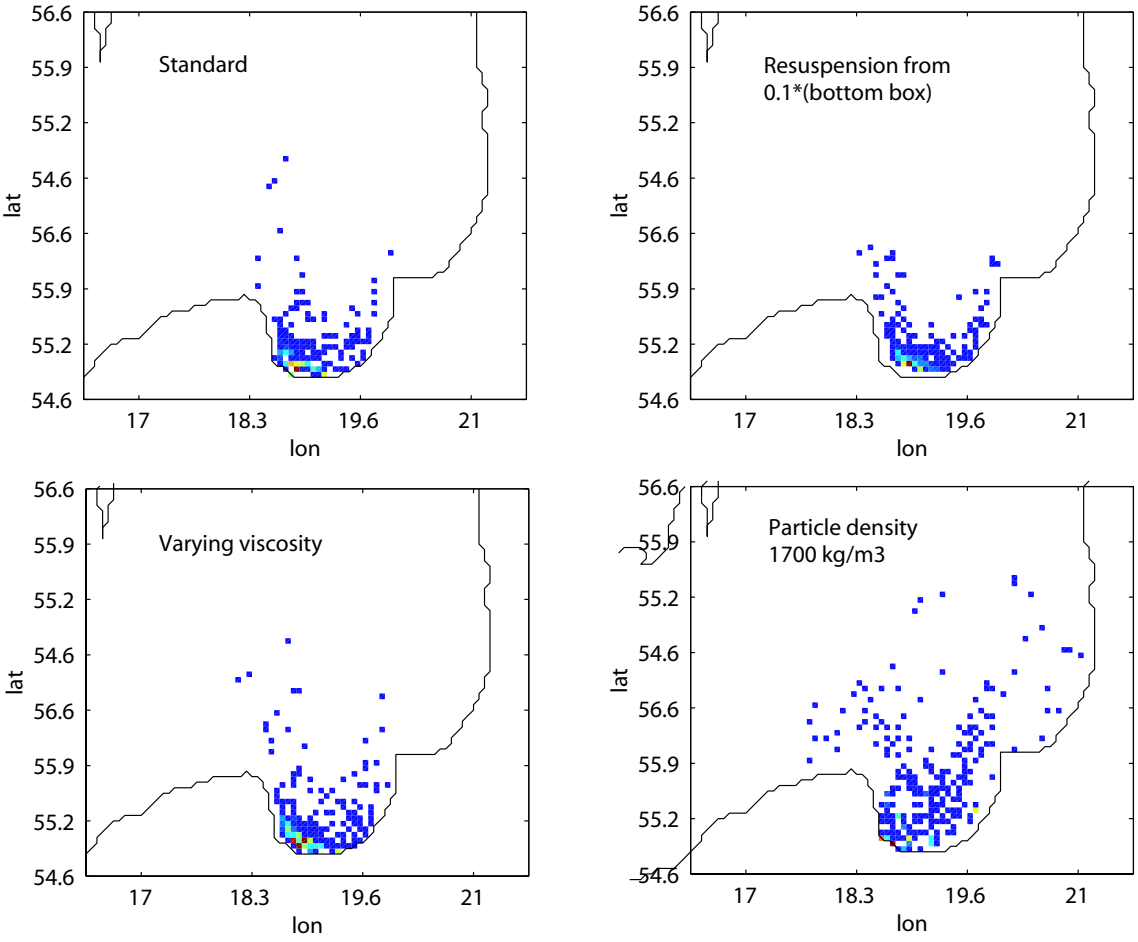


Figure 20: Results from sensitivity analysis, standard run top left.

Decreasing the particle density makes the particles travel a greater distance, as can be seen in figure 20, an expected result since the settling velocity decreases when the particle density increases, as can be seen in equation (12). A lower resuspension height decreases the distance the particles travel, also in figure 20. This is an expected result for a short simulation since the distance the particles can travel between every resuspension event gets shorter. Letting the viscosity vary with the temperature does not have a major effect on the medium-size silt particle, lower left in figure 20.

**Experiments with fine silt**

Different values for $u_{crit}$ were tested for fine silt. One lower value, 8 cm/s, and two larger, 15 and 20 cm/s, were tested. The difference between 8 cm/s, 15 cm/s and the standard was negligible. In the case with a $u_{crit}$ value of 20 cm/s a tendency towards less spreading could be seen, the particles still moved up northward, but they did not spread out in other directions as much.

A varying viscosity has a somewhat more visible effect on a lighter particle such as the fine silt, than on the medium silt. The movement up along the western coastline that can be seen in figure 18 is more pronounced in the run with the varying viscosity. The effect on clay would probably be even greater, but since most of the clay particles still are in suspension after 6 years the result are not clearly visible.

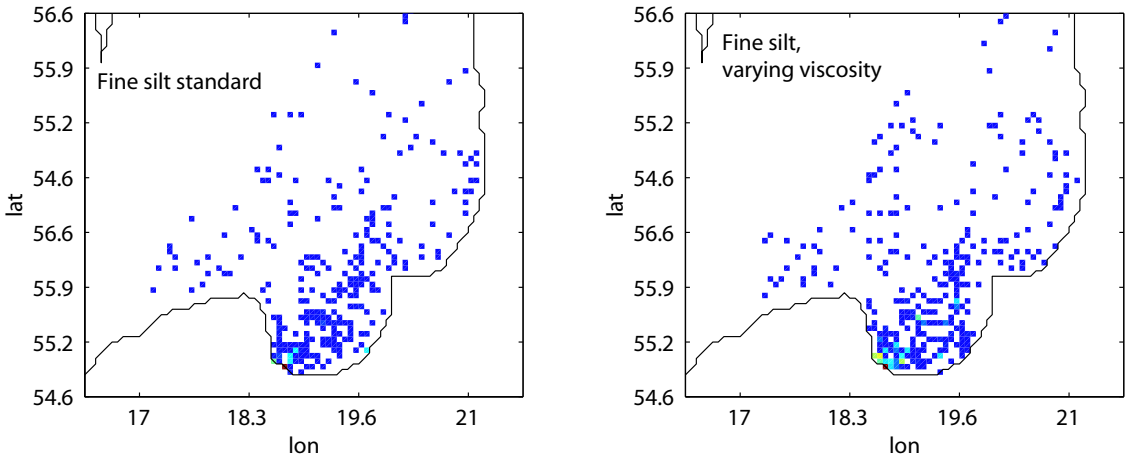


Figure 21: Runs with varying viscosity of water, standard fine silt to the left.

**Uncertainty in field data**

The results above show the sensitivity of the model to changes in input. This has to be correlated to the uncertainty in the field data to give any information about the true sensitivity. Figure 20 shows that the parameter with most influence is the density. Since this can be measured with good accuracy this is not a problem. The parameter with the greatest uncertainty of those tested is the resuspension height. This parameter did not have such a dramatic effect on the outcome, and the overall result is that the model is quite insensitive to reasonable changes in the input parameters.

# 5 DISCUSSION AND CONCLUSIONS

## 5.1 THE MAIN RESULTS

The results from the long simulation with clay shows good agreement with the map over bottom types in the Baltic proper. If areas with less than 15 particles are excluded, as in figure 15, none of the remaining clay particles seem to have ended up in areas not marked as clay on the map. As can be seen in comparison with figure 16, most clay is found in areas with a depth of 90 metres or more, and the particles tend to cluster at the edges, especially at the eastern slope of the Gotland deep. A small amount of the clay particles have made it all the way to the Bornholm deep. Since the circulation cell in the Baltic proper is directed counter clockwise around Gotland this suggests that they have traveled quite far to get there. The time series figure 17 support this theory.

Unfortunately the map does not include any distinction between different types of fine sediments and everything from medium silt to clay is in the same group. This means that the fine silt should have ended up in the same area as the clay, which it did not. Comparing the fine silt run with the full bottom map, figure 19, shows that the silt to some extent is found where there is supposed to be fine and medium sand. A longer simulation may show that the silt eventually will leave these areas. If the particles that are gathered along the eastern coastline continue northward they will probably end up in the area of coarse aleurit seen on the map, a more suitable place for them.

When attempting a more detailed study of the different areas on the sediment map and comparing them to the model results, the effect of the sand reefs should be considered. All the way along the west and south coast of the Baltic Proper the river outlets are shielded by sand reefs. This is one of the main reasons why Wisla was chosen as a model river, being the one large river least covered by a reef. The areas inside these reefs are not included in the RCO model, instead the river outlet through the reef serves as the outlet to the model area. Still these reefs and the lagoons inside of them may slightly alter the locations of the sediments in the coastal area, which should be considered as a possible source of error when comparing the model results to detailed maps.

## 5.2 THE SENSITIVITY ANALYSIS

**Variable viscosity**

The dynamic viscosity of water has a substantial impact on the settling velocity of particles with a diameter of 0.2 mm or smaller. The vertical velocity differs by more than 30% between water temperatures of 4°C and 20°C, see equation (12). Two ways to handle the viscosity are tested in this study. One is to calculate the velocity in the beginning of the simulation with an average value of the water viscosity. The other is to calculate the settling velocity for each particle trajectory at every time step from the temperature at the location of the particle. The question at hand was if a great difference in settling velocity necessarily gives a large difference in the outcome of the model, i.e. the final locations of the particles. As seen in section (4.2) the difference increased a little as the particles got smaller. Keeping in mind the calculation load added, it seems questionable to use the varying viscosity in the case with particles the size of medium silt and larger. For fine silt and smaller the better approximation of the settling velocity justifies the use, even though for both cases the final results of long enough simulations appear to be very much alike. Still, the viscosity approximation in the model is very crude, only a stepwise change between table values, and the salinity is not

accounted for. Calculating a more accurate value of the viscosity from the temperature and the salinity will add much more computer time to the simulations.

As an average value for the viscosity, that for pure water corresponding to a temperature of 10° Celsius was chosen. A seasonal variation in temperature only exists at a depth less than 100 metres, below that the temperature is stable at about 4°C. An average temperature of the Baltic Sea would not be as high as 10 degrees, but since the largest part of the sedimentation and resuspension events takes place at shallower depths, the choice seemed reasonable. The effect of the salt in the Baltic was ignored for the same reasons; even if the salinity in the deeper parts can be quite high, the surface water in the Baltic Proper only has a salinity of between 5 and 7.5 psu and it should not have an impact on the approximation greater than that of the temperature.

**Variations of $\alpha$ and T**

The model shows low sensitivity to changes in the parameters controlling the approximation of the orbital water velocity, provided that these are within reasonable limits. To test the sensitivity by making the parameters abnormally large or small seemed pointless since they are coupled in the equation. The lower $\alpha$-value used in the sensitivity analysis corresponds to a higher water velocity at the surface, estimated in section (3.3.3). This is not unlikely since the same lack of short waves in the RCO velocity field that makes the water velocity at the bottom too small to model sediment transport with should also make the velocity at the surface too small. Note that this is not an error in the RCO model, the water movements due to the short waves do not lead to a net transport between the grid boxes and are therefore not taken into accounted in that model.

The approximations made in the sedimentation model correspond to a sea with high waves with a constant period all the year round. This is unrealistic, but serves the purpose of transporting particles. The $\alpha$-value is correlated with the surface velocity from the RCO through $a = \alpha U(s)$. If the period time also in some way was connected to the momentary velocity at the surface, the approximation of the orbital velocity $u_a(bz)a$, see equation (25), would be more reasonable. Furthermore the variations in the water motion would be visible not only in the actual bottom box velocity $U(bz)$ from the RCO, but also in the approximative orbital velocity. An even better thing to do would be to couple the model with a proper wave model and thereby making the approximations unnecessary altogether since all the parameters in equation (23) then would be known. This is an improvement that will be necessary in the future.

**Different values for $u_{crit}$**

The standard $u_{crit}$ was set to 0.10 m/s for all particle sizes tested. This roughly corresponds to the values given by Postma and Hjulström and the model seems rather insensitive to small changes in $u_{crit}$ around this value. The resuspension events are however controlled not only by the value of $u_{crit}$, but also by the total velocity at the bottom and thereby the approximation of the orbital water velocity. Too small a $u_{crit}$ can be balanced by too large an orbital velocity and vice versa.

As can be seen in figure (13) the critical velocity for silt and clay is dependent on the water content. A smaller water content makes the cohesive forces between the particles stronger and the critical velocity gets larger. Since it in the sedimentation model is assumed that each particle always is free to move, i.e. it will not be covered by other particles, the water content is assumed to be 100%.

**The resuspension height**

Decreasing the resuspension height made the distance traveled by the medium silt particles after six years of simulation visibly shorter, as seen in figure (20). In the upper 99 metres of the sea the depth of each box is 3 metres, and the standard resuspension height is 1.5 metres. The decreased height was 0.3 metres. I have found no published value of the average resuspension height of fine particles in open water, but the common prejudice seems to be towards the lower value. The result will probably be the same if the simulation time is long enough.

## 5.3 ABOUT THE SEDIMENTATION MODEL

**Larger particles and balancing errors**

All particles studied and discussed here are very small, a fact that is emphasized by the sediment map grouping them all together. Larger particles tested in the model gave a very poor result. For example a run with fine sand, diameter 0.06 mm, did not leave the first two grid cells outside Wisla. The enormous data files generated suggested that they were "jumping around", but never stayed suspended long enough to make it anywhere. Since the model does not handle rolling, the coarser particles are missing their main form of transportation. A lower resuspension height can simulate small saltation jumps and might be an option for these particles, but the spatial resolution is still too coarse. Even if the particles make it to their mapped destination, the travel distance is very short compared to that of the finer particles.

No long simulation with numerous particles is made for medium silt, but it would probably be similar to the ones from the sensitivity analysis. Based on their small mass both the fine and the medium silt should travel further than they in fact do. This serves as a hint that they either fall to fast or do not become resuspended to the expected degree. Right now the settling velocity is the best modeled parameter, the only approximation here being the one for the viscosity. Still it seems that the particles settle too fast. If an almost correct vertical velocity is not balanced by an equally correct horizontal one, the former may appear wrong. Maybe the same sloshing that controls the resuspension also plays a part in the actual transport of the particles? These motions does not lead to a net transport of water between grid cells, apart from the marginal Stokes drift, but is this necessarily true for constantly resuspending particles? Anyhow, determining which parameters that are too large or too small separately when all parameters are interconnected is a difficult task. The errors tend to balance each other, and with the time dependence things get even more complex to sort out; the correct result may be reached but at the wrong time. If the final positions are the main issue, this may be irrelevant. If the settling velocity in fact is to large compared to the other model parameters, then possibly the results for one particle size in fact constitute the proper results for a larger particle. The clustering of the finer particles on the map gives no clues in this matter.

**Lagrangeian trajectory modelling**

This sedimentation model is based on the assumption that the sediment particles will travel along with the water while they sink. Assuming that we can model the sedimentation and resuspension processes perfectly we still need a certain accuracy of the water trajectories for the sediment to end up where it is supposed to.

Using Lagrangian trajectories instead of more conventional advection/diffusion models eliminates the problem with numerical diffusion, which otherwise decreases the positional accur-

acy (Gidhagen et al., 1989). Still trajectory computations have several sources of error, not only numerical ones such as those due to truncation, but also errors caused by differences between simulated and actual velocity fields and the interpolation in time and space (Seibert, 1992). Studies of atmospheric trajectory models have shown average deviations of 10 - 30% of the travel distance, mainly due to interpolation errors related to the vertical velocity (Baumann and Stohl, 1996). This makes a great difference when following a few specific objects, such as hot air balloons, but may not have such a dramatic influence on the outcome of a more statistically oriented study with thousands of objects. Either way, the overall accuracy of the sedimentation model can never exceed the accuracy of the water trajectory model and the RCO.

**Other applications**

The ability to follow individual particles as they move with the water gives rise to several new possible applications other than sedimentation modelling. The motion of plankton and the connection between the location of the blooming colonies and the nutrient transport in the sea is one example. The travel route of clam larvae and the optimal location for new cultivation areas is another. The ability to follow the chemical discharges from known point sources provides a tool for better estimations of the potential damage.

## 5.4 CONCLUSIONS

- Large-scale modeling of sedimentation processes with advective water trajectories based on velocity fields from circulation models has good potential to become a useful tool in sediment research.
- The model gives good results for clay, while it for the fine silt does not behave satisfactorily yet. As for medium and coarse silt the model should be able to model them since they are capable of travelling some distance due to their small size. Coarser particles do not travel far enough in relation to grid resolution and it makes no sense trying to model them with this large-scale model.
- To provide better estimations the model needs to be supplemented with a wave model. This would enable a proper parametrization of the orbital velocity, and thereby maybe come to terms with the unsatisfactory results for the larger of the fine particles.
- To improve future validation more sediment data is needed, preferably data that can be treated with Geographical Information System software.
- If long simulations with numerous particles are to be done the model would gain by being parallelized to shorten the computation time.
- The model may have its shortcomings, but it also has a great strength in the possibility to follow individual particles from different starting points under different conditions. The best way to make use of the model is to ask the questions that the model can answer. It may be possible to make a better model that can answer more questions, but that does not prevent the use of this one to the extent of its capabilities.

# References


Arakawa, A. and Mesinger, F., (1976), *Numerical Methods Used in Atmospheric Models.* GARP Publications Series, World Meteorological Organization.

Bryan, K., (1969), A numerical method for the study of circulation in the world ocean. *Journal of Computaional Physics*,4:3, 347–376.

Baumann, K. and Stohl, A., (1996), Validation of a Long-Range Trajectory Model Using Gas Balloon Tracks from the Gordon Bennett Cup 95. *Journal of Applied Meteorology*, 36, 711–720.

Christiansen, C., Gertz, F., Laima, M. J.,Lund-Hansen, L. C., Vang, T. and Jürgensen, C., (1997), Nutrient (P,N) dynamics in the southwestern Kattegat, Scandinavia: sedimentation and resuspension effects. *Journal of Marine Systems*, 29, 66–77.

Cox, M. D., (1984), *GFDL Ocean Group Thecnical report.* Geophysical Fluid Dynamics Laboratory/NOOA, Princeton University. 1, 143pp.

Draxler, R. R., (1996), Trajectory Optimization for Ballon Flight Planning. *Weather and Forecast*, 11:1, 111–114.

Döös, K., (1995), Interocean exchange of water masses. *Journal of Geophysical Research*, 100, 499–514.

Döös, K., Meier, H. E. M. and Döscher, R., (2004) The Baltic Haline Conveyor Belt, or The Overturning Circulation and Mixing in the Baltic. *Ambio*, 33:4–5, 261–266.

Döös, K. and De Vries, P., (2000), Calculating Lagrangeian Trajectories Using Time-Dependent Velocity Fields. *Journal of Atmospheric and Ocean Technology*, 18, 1092–1101.

FRP, (1978), *The sea; natural conditions and use.* Fysisk riksplanering (FRP), Bostadsdepartementet, No. 7, 303 p.

Gibbs, R. J., Matthews, M. D. and Link, D. A., (1971), The relationship between sphere size and settling velocity. *Journal of Sedimentary Petrology*, 14, 7–18.

Gidhagen, L., Rahm, L. and Nyberg, L., (1989), Lagrangian modelling of dispersion, sedimentation and resuspension processes in marine environments. *Dt. Hydrogr. Z.*, 42, 249–270.

Helsinki Comission, (2004), *Excecutive Summary of the Fourth Baltic Sea Pollution Load Compilation.* Baltic Marine Environment Protection Commission, Helsiniki, Finland.

Heynsfield, A. J., (1983), Case Study of a Hailstorm in Colorado. Part IV: Graupel and Hail Growth Mechanisms Deducted through Particle Trajectory Calculations. *Journal of Athmospheric Sciences*, 40:6, 1482–1509.

Hibler, W. D., (1979), A Dynamic and Thermodynamic Sea Ice Model. *Journal of Physical Oceanography*, 9, 817–846.

Hjulström, F., (1935), The morphological activity of rivers as illustrated by river Fyris. Bulletin of the Geological Institute Uppsala, 30:25, 211–527.

Håkanson, L. and Wallin, M., (1992), Morphometry and sedimentation as regulating factors for nutrient recykling and trophic state in coastal waters. *Hydrobiologia*, 236/236, 33–45.

Håkanson, L. and Floderius, S., (1989), Resuspension, ephemeral mud blankets and nitrogen cycling Laholmsbukten, south Kattegat. *Hydrobiologia*, 176/177, 1101–1110.

Jonsson, P., Carman, P. and Wulff, F., (1990), Laminated Sediments in the Baltic - A tool for Evaluating Nutrient Mass Balances. *Ambio*, 19:3, 152–158.

Jönsson, A., (2001), *The Baltic Sea Wave Filed, Impacts on Sediment and Biogeochemistry.* Departement of Water and Environmental Studies, University of Linköping, Licenciate Thesis.

Jönsson, B., Lundberg, P. and Döös, K., (2004), Baltic Sub-basin Turnover Times Examined Using the Rossby Centre Ocean Model. *Ambio*, 33:4–5, 257–261.

Komar, P. D. and Miller M. C., (1973), The treshold of sediment movement under oscillatory water waves. *Journal of Sedimentary Petrology*, 43:4, 1101–1110.

LTG, (1999), *LTG series of marine geological maps, No. 1.* Lithuanian Geological Survey (LTG).

Meier, H. E. M. and Faxén, T., (2001), Performance Analysis of a Multiprocessor Coupled Ice-Ocean Model for the Baltic sea. *Journal of Atmospheric and Oceanic Technology*, 19, 114–124.

Mysak, L. A. and LeBlond, P. H., (1978), *Waves in the Ocean.* Elselvier Oceanography Series, Elselvier Scientific Publishing Company.

Nielsen, P., (1992), *Coastal bottom boundary layers and sediment transport.* World Scientific Publishing Co. Pte. Ltd, Advanced Series on Ocean Engineering - Volume 4.

Nordling, C. and Österman, J., (1996), *Physics Handbook for Science and Engineering*, Studentlitteratur AB.

Pacanowski, R. C., and Griffies, S. M., (2000), *MOM 3.0 Manual.* Geophysical Fluid Dynamics Laboratory.

Pack, D. H., Ferber, G. J., Heffter, J. L., Telegadas, K., Angell, J. K., Hoecker, W. H. and Machta, L., (1978), Meteorology of long-range transport. *Atmospheric Enivironment*, 12, 425–444.

Postma, H., (1967), *Estuaries*: Sediment Transport and Sedimentation in the estuarine environment. American Association of Advancements in Science, Washington DC, pp158–179.

Samson, P. J., (1980), Trajectory Analysis of Summertime Sulfate Concentrations in the Northeastern United States. *Journal of Applied Meteorology*, 19:12, 1382–1394.

Seibert, P., (1992), Convergence and Accuracy of Numerical Methods for Trajectory Calculations. *Journal of Applied Metheorology*, 32, 558–566.

Seifert, T., Tauber, F. and Kayser, B., (2001), *A high resolution spherical grid topography of the Baltic Sea - revised edition.* Proceedings of the Baltic Sea Science Congress, Stockholm, 25-29 November 2001.

Semtner, A. J., (1974), *A general cirkulation model for the world ocean.* Departement of Meteorolgy, University of Calefornia. 9, 99pp.

SGU, (1999), *SGU series of geological maps, Ba No. 54.* Swedish Geological Survey (SGU).

Shepard, F. P. (editor), (1967), *Submarine geology.* Harper and Row, Chapter 5, Sediments: Physical properties and mechanics of sedimentation, by D. L. Inman.

Simon, N. S., (1989), Nitrogen cycling between sediments and the shallow-water column in the transition zone of the Pontomac river and estuary., II. The role of wind-driven resuspension and adsorbed ammonium. *Estuarine Coastal Shelf science*, 28, 531–547.

Sjöberg, B. (editor), (1992), *Sea and Coast.* Swedish National Atlas. SNA, Stockholm, 128pp. (In Swedish).

Stohl, A., (1996b), Trajectory Statistics -A new method to establish source-receptor relationships of air pollutatnt and its application to the transport of particulate sulfate in Europe. *Atmospheric Enivironment*, 30:4, 579–587.

Svensson, J. and Wickström, K., (1986), *Wave Data from Swedish Coastal Waters 1985.* Swedish Meterorological and Hydrological Institute, Oceanography departement, 8, (in swedish).

Sweizer, J., Langaas, S. and Folke, C., (1996), Land Cover and Population Density in the Balic Sea Drainage Basin: A GIS Database. *Ambio*, 25:3, 191–198.

Webb, D. J., de Cuevas, B. A. and Coward, A. c., (1998), *The first main run of the OCCAM global ocean model.* Southampton Oceanography Centre. 34.

Wu, L. and Wang, B., (2003), Assessing Impacts of Global Warming on Tropical Cyklone Tracks. *Journal of Climate*, 17:8, 1686–1698.